applied sciences

MDPI

Article

Evaluation of the Seismic Capacity of Existing Moment Resisting Frames by a Simplified Approach: Examples and Numerical Application

Rosario Montuori [1], Elide Nastri [2], Vincenzo Piluso [2] and Paolo Todisco [2,*]

[1] Department of Pharmacy, University of Salerno, 84084 Fisciano, SA, Italy; r.montuori@unisa.it
[2] Department of Civil Engineering, University of Salerno, 84084 Fisciano, SA, Italy; enastri@unisa.it (E.N.); v.piluso@unisa.it (V.P.)
* Correspondence: ptodisco@unisa.it

Abstract: The capacity of a structure can be assessed using inelastic analysis, requiring sophisticated numerical procedures such as pushover and incremental dynamic analyses. A simplified method for the evaluation of the seismic performance of steel moment resisting frames (MRFs) to be used in everyday practice has been recently proposed. This method evaluates the capacity of buildings employing an analytical trilinear model without resorting to any non−linear analysis. Despite the methodologies suggested by codes, the assessing procedure herein described is of easy application, also by hand calculation. Furthermore, it constitutes a suitable tool to check the capacity of the buildings designed with the new seismic code prescriptions. The proposed methodology has been set up through a large parametric analysis, carried out on 420frames designed according to three different approaches: the theory of plastic mechanism control (TPMC), ensuring the design of structures showing global collapse mechanism (GMRFs), the one based on the Eurocode 8 design requirements (SMRFs), and a simple design against horizontal loads (OMRFs) without specific seismic requirements. In this paper, some examples of the application of this simplified methodology are proposed with references to structures supposed to exhibit global, partial and soft storey mechanism.

Keywords: TPMC; pushovers; capacity; performances; vulnerability; simplified methods

Citation: Montuori, R.; Nastri, E.; Piluso, V.; Todisco, P. Evaluation of the Seismic Capacity of Existing Moment Resisting Frames by a Simplified Approach: Examples and Numerical Application. *Appl. Sci.* **2021**, *11*, 2594. https://doi.org/10.3390/app11062594

Academic Editor: Chiara Bedon

Received: 1 March 2021
Accepted: 11 March 2021
Published: 15 March 2021

1. Introduction

The safeguard of the built heritage is gaining an increasing interest in structural and seismic engineering [1,2]. The knowledge of the seismic response of the structures plays a fundamental role in the evaluation of the seismic vulnerability of existing structures [3–6] and in the prediction of the expected losses [7–9]. The designer, to achieve a correct safety evaluation in terms of the capacity demand ratio, must resort to non−linear models and non−linear analyses [10–13], which, even though they are described in the codes, are very prone to being misinterpreted. The implementation of a non−linear model needs adequate experience and, first of all, an adequate knowledge of the condition of the building to be modelled in terms of geometry, loads, structural details, materials and degradation [14–18]. In the perspective of a seismic classification of the built heritage, it is necessary to define a standardizable, unique and user−friendly methodology [19–22]; therefore, recently, a simplified assessment approach has been developed concerning steel moment resisting frames (MRFs) [23] based on a trilinear model that needs only the elastic structural analysis and the rigid-plastic analysis and does not require any static or dynamic non−linear effort. Rigid plastic analysis has generally been used as an assessment tool against vertical and horizontal loads. The novelty point of the procedure is to use the rigid plastic and elastic analysis joined with a performance-based evaluation aimed at easily assessing the seismic performance of existing buildings, also ensuring a rapid mapping of the built heritage in terms of seismic vulnerability.

This assessment procedure is herein applied to some study cases to support their ease of application. It mainly consists of the definition of a trilinear capacity curve by some characteristic points that define three branches [24,25]. These points correspond to different limit states. It is important to mention that the code assessment approach does not provide the definition of specific performance points on the pushover curve, thus entrusting the designer to the definition of required target limits which are provided by codes in terms of member chord rotation.

The method has been set up by performing several parametric analyses, in terms of pushovers, on 420 frames, designed according to three different approaches, i.e., without any seismic detailing (O−MRFs), by Eurocode 8 (S−MRFs) and by the theory of plastic mechanism control (G−MRFs). It is usually observed that structures designed without any seismic provision exhibit a soft storey mechanism while the structures designed according to the modern approach of Eurocode 8 can achieve more robust performances even if the global mechanism can be assured only by the TPMC approach. The results belonging to the pushover analyses performed on the structures have been used to calibrate the assessment relationships, ensuring a wide application of the method. The comparison in terms of capacity and demand can be made according to two alternative approaches: the one proposed by Eurocode 8 [26] and the one proposed by Nassar and Krawinkler [27]. The former exploits the concept of ADRS spectrum while the latter has the benefit of being of more easily applicable because it does not single out between low and high periods of vibration. In the following, the main model equations are reported and described.

2. Fundamental Equations of the Trilinear Model

The simplified trilinear model needs only the elastic structural analysis and the rigid-plastic analysis [28–31] not requiring any static or dynamic non-linear analyses. Therefore, the user can quickly obtain the capacity curve through the intersection of three linear branches (Figure 1), computed using simple relationships proposed in the following. Referring to the proposed model, the first branch of the curve can be approximated by the elastic response curve; the horizontal one is defined using the maximum load-bearing capacity given by the calibrated Merchant−Rankine formula, while, the softening branch is given by the collapse mechanism equilibrium curve of the structure, influenced by the second-order effects [32–36]. The definition of the third branch is linked to the concept of the mechanism equilibrium curve. In particular, the equation of the third branch can be obtained by equating the virtual internal work of the dissipative zones with the virtual external work of the structure, accounting for second-order effects.

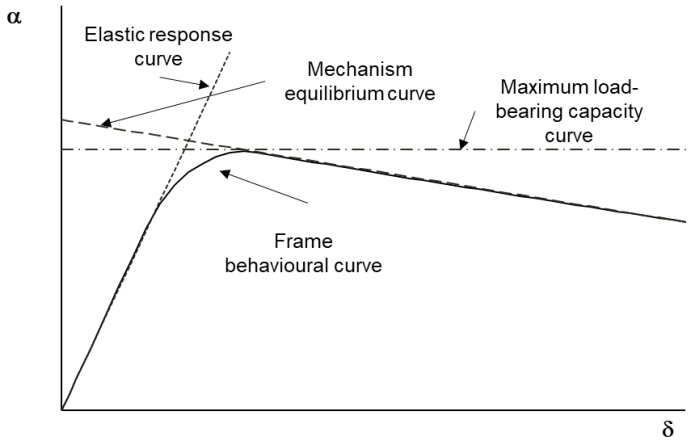

Figure 1. Trilinear approximation of the capacity curve.

The equations of the three identified branches in the $\alpha-\delta$ plane (horizontal force multiplier—top sway displacement) are reported below:

- Elastic response curve:

$$\alpha = \frac{1}{\delta_1}\delta \tag{1}$$

- Maximum load-bearing capacity curve according to the modified Merchant−Rankine formulation [23,37,38]

$$\alpha = \alpha_{max} = \frac{\alpha_0}{1 + \Psi\alpha_0\gamma_s\delta_1} \tag{2}$$

where:

$$\Psi = \alpha + b\xi \tag{3}$$

$$\xi = \frac{\sum \frac{EI_b}{L_b}}{\sum \frac{EI_c}{L_c}} \tag{4}$$

The use of Equation (3) is proposed by assuming for the coefficient Ψ with the following relation:

$$\Psi = 0.28488 - 0.14042\,\xi \tag{5}$$

- The mechanism equilibrium curve according to rigid-plastic analysis [37]:

$$\alpha = \alpha_0 - \gamma_s(\delta - \delta_y) \tag{6}$$

Characteristic performance points (points A, B, C, D of Figure 2) have been identified on the trilinear model. The points are associated with specific limit states [35], provided by codes, identifying a target performance level [34,39–41].

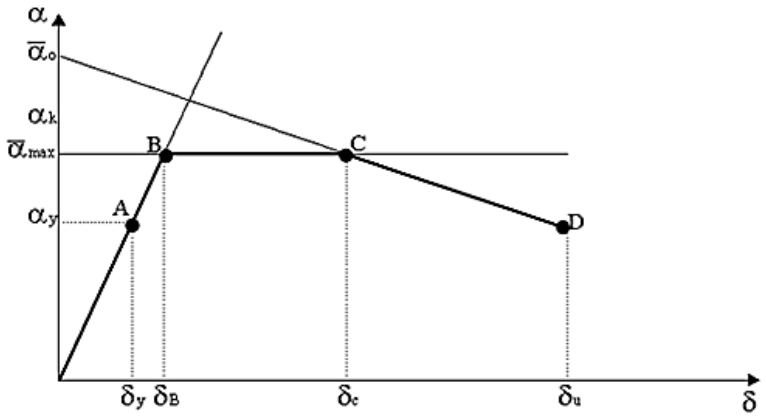

Figure 2. Characteristic performance points.

- Point A—"Fully Operational"

$$\alpha_A = \frac{1}{\delta_1}\delta_A \tag{7}$$

where δ_A is the displacement corresponding to the minimum between the displacement in the service conditions and δ_y is the displacement corresponding to the formation of the first plastic hinge.

- Point B—"Operational"

$$\alpha_B = \alpha_{max}\,;\ \delta_B = \alpha_{max}\delta_y \tag{8}$$

where α_{max} is the maximum multiplier defined according to the Equation (2).

- Point C—"Life Safety"

$$\alpha_C = \alpha_{max}\ ;\ \delta_C = \delta_{mecc} = \frac{\alpha_0 - \alpha_{max}}{\gamma_S} + \delta_y \tag{9}$$

This point derives from the intersection of the horizontal branch of equation $\alpha = \alpha_{max}$ with the softening branch, representative of the collapse mechanism equilibrium curve, of equation $\alpha = \alpha_0 - \gamma_S(\delta - \delta_y)$.

- Point D—"Near Collapse"

$$\alpha_D = \alpha_{max} - \gamma_s(\delta_D - \delta_C)\ ;\ \delta_D = \delta_C + \left(\vartheta_{\rho.\mu} - \vartheta_{\rho.mecc}\right)H_0 \tag{10}$$

The chord rotation at yielding ϑ_y is defined as a property of the member. For ductile elements and brittle elements involved into soft-storey mechanisms, are given by:

$$\vartheta_y = \frac{\gamma_{ov} M_{p.m} l_m}{6EI_m} \tag{11}$$

while for brittle elements involved in partial and global mechanisms:

$$\vartheta_y = \frac{\gamma_{ov} M_{p.m} l_m}{4EI_m} \tag{12}$$

For the evaluation of plastic rotations occurring in the critical members, an analytical formulation is proposed, based on a "shear−type" single−storey portal with different plastic moments at the top and base of the columns. The relationships for the evaluation of the plastic rotation demand corresponding to the development of the collapse mechanism are reported as follows:

$$\frac{\theta_{p.mec}\ H_0}{n_s \delta_y} = \frac{\Psi_1}{\Psi_2}\Psi_3\left(\frac{\alpha_{max}}{\alpha_y} - 1\right)^{\Psi_4}\frac{1 - \Psi_5\gamma_s}{1 - \Psi_6\gamma_s} \tag{13}$$

$$\frac{\theta_{p.mec}\ H_0}{n_s \delta_y} = \frac{\Psi'_1}{\Psi'_2}\Psi_3\left(\frac{\alpha_{max}}{\alpha_y} - 1\right)^{\Psi'_4}\frac{1 - \Psi'_5\gamma_s}{1 - \Psi'_6\gamma_s} \tag{14}$$

In particular, the coefficient with the apex refers to the element achieving the collapse (i.e., the critical element), with those without the apex to the element developing the first yielding.

The Ψ_i coefficients to be used in Equations (13) and (14), are given by the following equations whose parameters are reported in Table 1:

$$\Psi_1 = \alpha_1 + b_1 n_b \qquad \Psi'_1 = \alpha'_1 + b'_1 n_b \tag{15}$$

$$\Psi_2 = \alpha_2 + b_2 n_s \qquad \Psi'_2 = \alpha'_2 + b'_2 n_s \tag{16}$$

$$\Psi i = \alpha i + bi\xi \quad i = 3,\ldots,6 \qquad \Psi' i = \alpha' i + b' i\xi \quad i = 3,\ldots,6 \tag{17}$$

Table 1. Regression coefficients for the evaluation of plastic rotation demand for the development of the collapse mechanism.

	GMRFs	SMRFs	OMRFs
a1	2.7747755	2.982417	19.542818
b1	0.0207354	−0.14356	−1.372652
a2	1.817070	1.370201	−144.9099
b2	−0.07731	0.652663	123.8454
a3	0.0844528	0.964755	−0.028950
b3	1.616165	1.802312	0.1820582
a4	−0.112433	0.737624	−1.840828
b4	1.4966937	−0.51209	3.0361764

Table 1. *Cont.*

	GMRFs	SMRFs	OMRFs
a5	1.0606602	0.976295	97.159963
b5	0.6787599	1.027818	25.416893
a6	1.0528759	0.975839	1.8666626
b6	0.7200734	1.030732	−0.429104
a′1	1.1674452	3.415537	19.508374
b′1	0.0575325	−0.07355	−0.637701
a′2	6.0112325	0.251316	−89.8716
b′2	0.3665074	1.394603	73.87363
a′3	1.0944684	3.860496	−0.044146
b′3	−1.169347	−0.09045	0.3181349
a′4	−2.322765	1.415893	−2.345411
b′4	7.462743	−1.18406	3.917804
a′5	0.993180	0.968454	−17.06279
b′5	0.95649	1.11087	95.899727
a′6	1.0150939	0.976968	1.5715063
b′6	0.7912074	1.069351	−0.053770

3. Assessment Procedure in Terms of Spectral Accelerations According to ADRS Spectrum

The capacity-demand assessment procedure can be expressed through the ADRS spectrum [12,26]. For each limit state, the spectrum $S_\alpha - S_{De}$ is defined by the means of the relationship $S_{De}(T) = S_\alpha(T)(T/2\pi)^2$. As regards the capacity, it is necessary to represent the characteristic points of the behavioral curve of the structure, in the ADRS plane. Of these points, it is necessary to know the abscissa, which is the displacement $d^*_{\mathrm{LS}} = d_{\mathrm{LS}}/\Gamma$.

It is necessary to distinguish between cases $T^* > T_C$ and $T^* < T_C$. If $T^* > T_C$ 41, the capacity in terms of spectral acceleration relative to the limit state considered can be obtained through the following relationship:

$$S_{aSL} = d^*_{LS}\omega^{*2}_0 \tag{18}$$

The demand is represented by the spectral acceleration provided by the code, for the specific limit state, in the case of the equivalent SDOF system with the equivalent period of vibration T^*.

For the assessment procedure, the inequality $S_{\alpha ls} \geq S_\alpha(T^*)$ must be satisfied.

If $T^* < T_C$ and $q > 1$, according to the equality energy criterion, there is a different procedure to evaluate the capacity that leads to the anelastic spectrum whose parameters are listed below:

$$F^*_{lS} = \frac{m^* S_a(T^*)}{q_{lS}} \tag{19}$$

$$q_{lS} = 1 + (\mu_{lS} - 1)\frac{T^*}{T_C} \tag{20}$$

$$S_{aSL} = q_{lS}\frac{F^*_{lS}}{m^*} \tag{21}$$

If $T^* < T_C$ and $q \leq 1$, it results:

$$F^*_{SL} = m^* S_a(T^*) \tag{22}$$

$$S_{aSL} = \frac{F^*_{lS}}{m^*} \tag{23}$$

$$m^* = \sum_{k=1}^{n} m_k F_k \tag{24}$$

The checking is verified when the inequality $S_{\alpha ls} \geq S_\alpha(T^*)$ is satisfied.

4. Assessment Procedure in Terms of Spectral Accelerations According to Nassar and Krawinkler

In the framework of capacity-demand checking [27,37–43], an equivalent SDOF system replaces the MDOF actual system by means of the modal participation factor Γ. Multiplying the multiplier α with the design base shear, the capacity curve is reported in an F_b—d_c plane. The capacity curve must be reduced through the modal participation factor and represented in an F^*—d^* plane. The demand is estimated through the period T^* and the equivalent mass m^* according to European codes. The capacity in terms of spectral acceleration for the points A, B, C, and D is given as follows:

- Point A—"Fully Operational"

$$S_{aFO}(T^*) = \frac{F^*_{FO}}{m^*} \tag{25}$$

- Point B—"Operational"

$$S_{aO}(T^*) = \frac{F^*_{O}}{m^*} \tag{26}$$

- Point C—"Life Safety"

$$S_{aLS}(T^*) = \frac{F^*_{LS}}{m^*} q_{LS} \tag{27}$$

$$q_{LS} = q_0(\mu, T, \gamma = 0) = [c(\mu_{LS} - 1) + 1]^{1/c} \tag{28}$$

where $c = \frac{T*}{1+T*} + \frac{0.42}{T*}$ and $\mu_{LS} = \frac{d_{LS}*}{d_0*}$.

- Point D—"Near Collapse"

$$S_{aNC}(T^*) = \frac{F^*_{NC}}{m^*} q_{NC} \tag{29}$$

$$q_{NC} = \frac{q_0}{\varphi} \tag{30}$$

$$q_0(\mu, T, \gamma = 0) = [c(\mu_{LS} - 1) + 1]^{1/c} \tag{31}$$

where $c = \frac{T*}{1+T*} + \frac{0.42}{T*}$ and $\mu_{NC} = \frac{d_{NC}*}{d_o*}$.

$$\varphi = \frac{1 + 0.62(\mu_{NC} - 1)^{1.45}\gamma}{(1 - \gamma)} \tag{32}$$

The coefficient φ is a function of the ductility μ and the non-dimensional slope of the equilibrium curve γ.

5. Numeric Example

The assessment procedure described above is applied to evaluate the capacity of a seven-storey and four-span steel moment resisting frame. The permanent loads G_k are equal to 3.5 kN/m^2 while the live loads Q_k equal 3 kN/m^2. For the evaluation of gravitational loads on the beams, a frame tributary length of 6.00 m has been set. The steel used is S275. In Figure 3a, a flowchart of the procedure is reported.

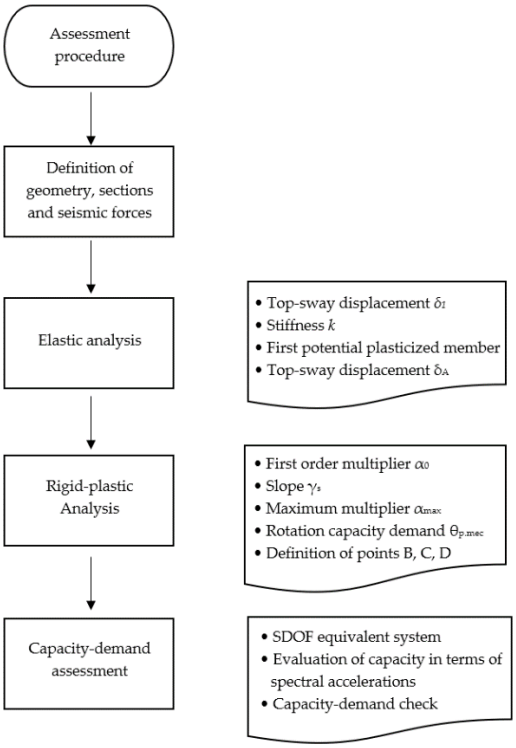

Figure 3. Flowchart of the assessment procedure.

5.1. Ordinary Moment Resisting Frame

Ordinary moment resisting frames are designed without any seismic prescription. The beams and column sections are reported in Figure 4.

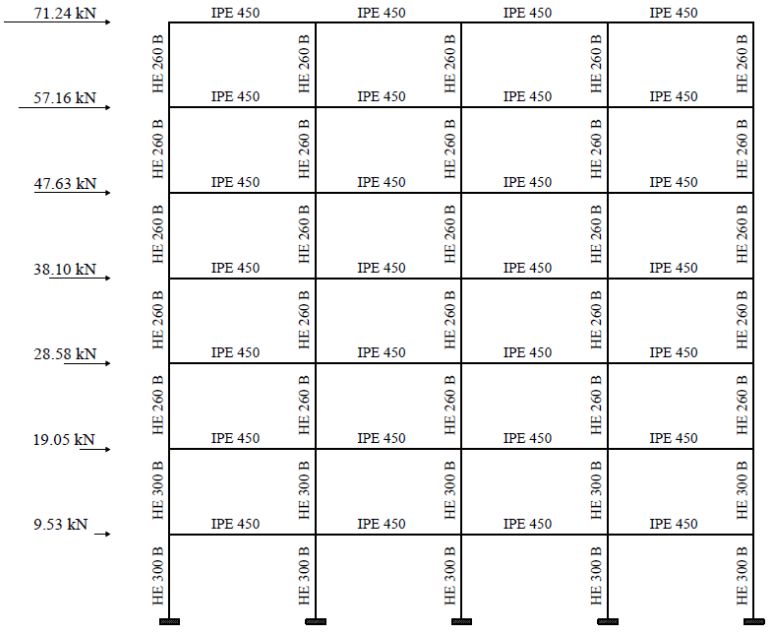

Figure 4. Diagram of the frame constituting the numeric example with indication of beams, columns and seismic forces.

The trilinear capacity curve is shown in Figure 5, which also shows the characteristic performance points of the model.

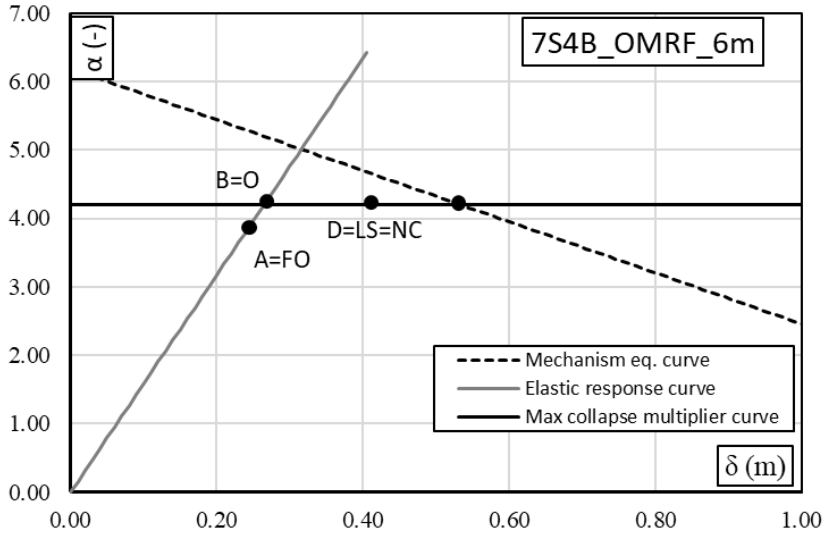

Figure 5. Trilinear model and characteristic points for the structure 7S4B_OMRF_6m.

Parameters obtained from the elastic analysis:

- $\delta_1(\alpha = 1) = 0.06305$ m
- $k = 15.8605\ \mathrm{m}^{-1}$
- $\delta_A = \delta_y = 0.2602$ m
- $\alpha_A = \alpha_y = k\delta_y = 4.128$

Parameters obtained from the rigid-plastic analysis:

- $\alpha_0 = 5.219$
- $\gamma_s = 3.729\ m^{-1}$
- $\alpha = \alpha_0 - \gamma_S(\delta - \delta_y) \rightarrow \alpha = 5.219 - 3.729(\delta - 0.2602)$
- $\alpha(\delta = 0) = \alpha_0 + \gamma_s\delta_y = 6.1888$
- $H_0 = 3.5\ m$(collapse mechanism Type 3, $i_m = 3$)

Evaluation of the maximum multiplier using the calibrated Merchant−Rankine formula:

- $$\alpha_{max} = \frac{\alpha_0}{1 + \Psi\alpha_0\gamma_s\delta_1} = 4.2025$$

where:

$$\Psi = 0.28488 - 0.14042\,\xi = 0.1970 \text{ with } \xi = \frac{\sum \frac{EI_b}{L_b}}{\sum \frac{EI_c}{L_c}} = 0.6255$$

and consequently $\delta_B = \frac{\alpha_{max}}{k} = 0.265$ and $\delta_c = \delta_{mecc} = \frac{\alpha_0 - \alpha_{max}}{\gamma_s} + \delta_y = \frac{5.219 - 4.2025}{3.729} + 0.2602 = 0.5326\ m$.

Evaluation of the plastic rotation demand corresponding to the development of the collapse mechanism for the first plasticized element (first storey beams):

- $$\theta_{p.mec} = \frac{n_s\delta_y}{H_0}\left[\frac{\Psi_1}{\Psi_2}\Psi_3\left(\frac{\alpha_{max}}{\alpha_y} - 1\right)^{\Psi_4}\frac{1 - \Psi_5\gamma_s}{1 - \Psi_6\gamma_s}\right] = 0.06612 \text{ rad}$$

The calculation of the corresponding capacity provides a final plastic rotation value of $8\theta_y = 8 \times 0.008257 = 0.06605$ rad.

Evaluation of the plastic rotation demand corresponding to the development of the collapse mechanism for the critical element (the mechanism is partial type 3 $i_m = 3$, so the critical element is a third storey column):

- $$\theta_{p.mec} = \frac{n_s \delta_y}{H_0}\left[\frac{\Psi'_1}{\Psi'_2}\Psi'_3\left(\frac{\alpha_{max}}{\alpha_y} - 1\right)^{\Psi'_4}\frac{1 - \Psi'_5\gamma_s}{1 - \Psi'_6\gamma_s}\right] = 0.07693 \text{ rad}$$

The calculation of the corresponding capacity, in the case of the third storey columns, provides a value of the ultimate plastic rotation equal to $8\theta_y = 8 \times 0.005568 = 0.04454$ rad. Therefore, the ultimate conditions are governed by the columns of the third storey.

Considering the plastic rotation capacity, the ultimate displacement is given by:

$$\delta_u = \delta_C + (\delta_{p.u} - \delta_{p.mecc})H_0 = 0.5326 + (0.04454 - 0.07693) \times 3.5 = 0.4192\, m$$

Since the plastic rotation capacity of the third storey columns is lower than that necessary for the complete development of the kinematic mechanism, the points C and D corresponding to the limit states "Life Safety" and "Near Collapse" are coincident and correspond to the aforementioned last displacement (δ_u).

All the verification procedures considered the use of the transformation of the MDOF system into an equivalent SDOF system using the participation coefficient of the main vibration mode Γ. For this reason, it is necessary to define:

- The eigenvector $\underline{\phi} = \{\phi_1, \phi_2, \phi_3, \phi_4, \phi_5, \phi_6\}$ that, assuming $\phi_k = \frac{F_k}{F_n}$, is:

$$\phi_1 = 0.134\, \phi_2 = 0.267\, \phi_3 = 0.401$$
$$\phi_4 = 0.535\, \phi_5 = 0.669\, \phi_6 = 0.802\, \phi_7 = 1.000$$

The modal participation factor Γ:

$$\Gamma = \frac{\sum_{k=1}^{n} m_k F_k}{\sum_{k=1}^{n} m_k {F_k}^2} = 1.4381$$

being:

$$m_1 = 57.98 \times 10^3 \text{ kg } m_2 = 57.98 \times 10^3 \text{ kg } m_3 = 57.98 \times 10^3 \text{ kg}$$
$$m_4 = 57.98 \times 10^3 \text{ kg } m_5 = 57.98 \times 10^3 \text{ kg } m_5 = 57.98 \times 10^3 \text{ kg } m_7 = 61.94 \times 10^3 \text{ kg}$$

The dynamic parameters of the equivalent SDOF system are reported in Table 2.

Table 2. Dynamic parameters of the equivalent SDOF system.

m*	***k****	***ω****	***T****
[kg 10^3]	[kN/m]	[rad/s]	[s]
224.76	**4302.8**	**4.3753**	**1.436**

Therefore, the characteristic points of the capacity curve are defined in the planes $\alpha - \delta$, $F_b - d_c$, $F^* - D^*$, $S_\alpha - S_D$ assessing the capacity in terms of accelerations for the Nassar and Krawinkler approach and ADRS spectrum approach. In Table 3, the results based on the use of the ADRS spectrum, and in Table 4, the results based on the use of the Nassar and Krawinkler formulation, are reported. The numbers in bold identify the values of spectral acceleration and displacement to be used in the capacity-demand assessment procedure.

Table 3. ADRS spectrum approach.

	FO	O	LS	NC
F [kN]	1119.90	1140.12	1140.12	1140.12
F^* [kN]	778.72	792.78	792.78	792.78
d [m]	0.2602	0.265	0.4192	0.4192
d^* [m]	**0.181**	**0.184**	**0.291**	**0.291**
Sa^* [g]	**0.353**	**0.359**	**0.569**	**0.569**

Table 4. Nassar and Krawinkler approach.

	FO	O	LS	NC
F [kN]	1119.90	1140.12	1140.12	1140.12
F^* [kN]	778.72	792.78	792.78	792.78
d [m]	0.2602	0.265	0.4192	0.4192
d^* [m]	**0.181**	**0.184**	**0.291**	**0.291**
μ [m]	–	–	1.582	1.582
Sa^* [g]	**0.353**	**0.359**	**0.575**	**0.575**

Seismic performance verification requires that, for each limit state, the inequality $S_{\alpha.ls}(T^*)_{capacity} \geq S_{\alpha.ls}(T^*)_{demand}$ is satisfied.

5.2. Special Moment Resisting Frame

Special moment resisting frames are designed to fulfil the Eurocode 8 seismic provisions. The selected case study with the definition of the beam and column dimension is reported in Figure 6.

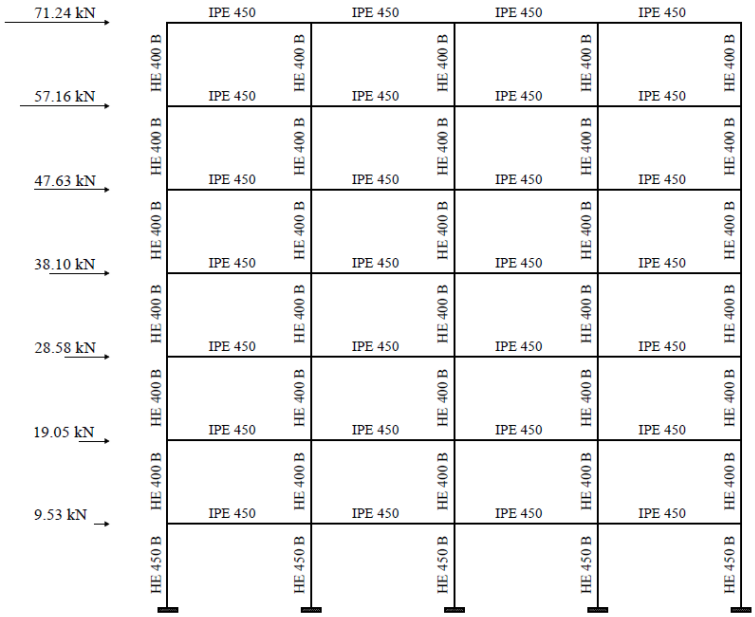

Figure 6. Diagram of the frame constituting the numeric example with the indication of beams, columns and seismic forces.

The trilinear capacity curve is shown in Figure 7, which also shows the characteristic performance points of the model.

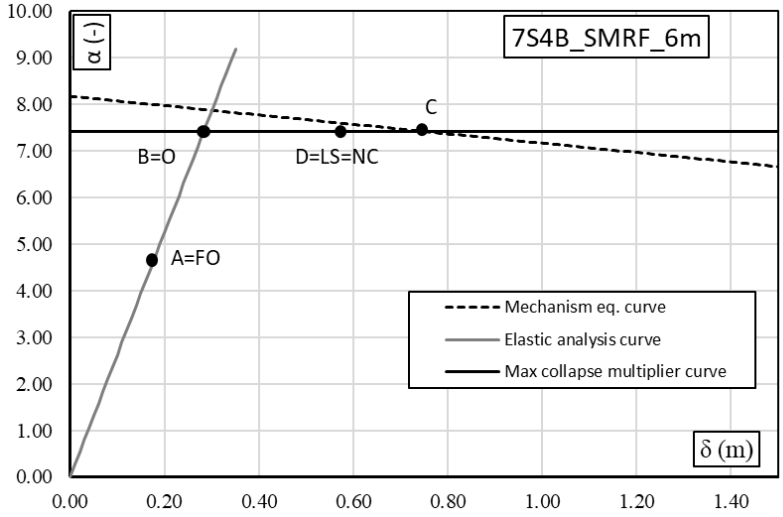

Figure 7. Trilinear model and characteristic points for the structure 7S4B_SMRF_6m.

Parameters obtained from the elastic analysis:

- $\delta_1(\alpha = 1) = 0.03814\ m$
- $k = 15.8605\ m^{-1}$
- $\delta_A = \delta_y = 0.1802\ m$
- $\alpha_A = \alpha_y = k\delta_y = 4.736$

Parameters obtained from the rigid-plastic analysis:

- $\alpha_0 = 7.989$
- $\gamma_s = 1.006\ m^{-1}$
- $\alpha = \alpha_0 - \gamma_s(\delta - \delta_y) \rightarrow \alpha = 7.989 - 1.006(\delta - 0.1802)$
- $\alpha(\delta = 0) = \alpha_0 + \gamma_s\delta_y = 8.1704$
- $H_0 = 14.0\ m$ (collapse mechanism Type 1, $i_m = 4$)

Evaluation of the maximum multiplier using the calibrated Merchant−Rankine formula:

- $$\alpha_{max} = \frac{\alpha_0}{1 + \Psi\alpha_0\gamma_s\delta_1} = 7.4056$$

where:

$$\Psi = 0.28488 - 0.14042\,\xi = 0.2572 \text{ with } \xi = \frac{\sum \frac{EI_b}{L_b}}{\sum \frac{EI_C}{L_c}} = 0.1971$$

and consequently $\delta_B = \frac{\alpha_{max}}{k} = 0.2824$ and $\delta_C = \delta_{mecc} = \frac{\alpha_0 - \alpha_{max}}{\gamma_s} + \delta_y = \frac{7.989 - 7.4056}{1.006} + 0.1802 = 0.7605\ m$.

Evaluation of the plastic rotation demand corresponding to the development of the collapse mechanism for the first plasticized element (first storey beams):

- $$\theta_{p.mec} = \frac{n_s\delta_y}{H_0}\left[\frac{\Psi_1}{\Psi_2}\Psi_3\left(\frac{\alpha_{max}}{\alpha_y} - 1\right)^{\Psi_4}\frac{1 - \Psi_5\gamma_s}{1 - \Psi_6\gamma_s}\right] = 0.03043 \text{ rad}$$

The calculation of the corresponding capacity provides a final plastic rotation value of $8\theta_y = 8 \times 0.008257 = 0.06605$ rad.

Evaluation of the plastic rotation demand corresponding to the development of the collapse mechanism for the critical element (the mechanism is partial type 1 $i_m = 4$, so the critical element is a first storey column):

•

$$\theta_{p.mec} = \frac{n_s \delta_y}{H_0}\left[\frac{\Psi'_1}{\Psi'_2}\Psi'_3\left(\frac{\alpha_{max}}{\alpha_y} - 1\right)^{\Psi'_4}\frac{1 - \Psi'_5\gamma_s}{1 - \Psi'_6\gamma_s}\right] = 0.04587 \text{ rad}$$

The calculation of the corresponding capacity, in the case of the third storey columns, provides a value of the ultimate plastic rotation equal to $8\theta_y = 8 \times 0.004212 = 0.033699$ rad. Therefore, the ultimate conditions are governed by the columns of the first storey.

Considering the plastic rotation capacity, the ultimate displacement is given by:

$$\delta_u = \delta_C + (\vartheta_{p.u} - \vartheta_{p.mecc})H_0 = 0.76 + (0.033699 - 0.04587) \times 14.0 = 0.5901\ m$$

Since the plastic rotation capacity of the third storey columns is lower than that necessary for the complete development of the kinematic mechanism, the points C and D corresponding to the limit states "Life Safety" and "Near Collapse" are coincident and correspond to the aforementioned last displacement (δ_u).

All the verification procedures considered the use of the transformation of the MDOF system by means of the participation coefficient of the main vibration mode Γ. For this reason, it is necessary to define:

The eigenvector $\underline{\phi} = \{\phi_1, \phi_2, \phi_3, \phi_4, \phi_5, \phi_6\}$that, assuming $\phi_k = \frac{F_k}{F_n}$, is:

$$\phi_1 = 0.134\ \phi_2 = 0.267\ \phi_3 = 0.401$$

$$\phi_4 = 0.535\ \phi_5 = 0.669\ \phi_6 = 0.802\ \phi_7 = 1.000$$

The modal participation factor Γ:

$$\Gamma = \frac{\sum_{k=1}^{n} m_k \phi_k}{\sum_{k=1}^{n} m_k {\phi_k}^2} = 1.4381$$

being:

$$m_1 = 57.98 \times 10^3 \text{ kg}\ m_2 = 57.98 \times 10^3 \text{ kg}\ m_3 = 57.98 \times 10^3 \text{ kg}$$

$$m_4 = 57.98 \times 10^3 \text{ kg}\ m_5 = 57.98 \times 10^3 \text{ kg}\ m_5 = 57.98 \times 10^3 \text{ kg}\ m_7 = 61.94 \times 10^3 \text{ kg}$$

The dynamic parameters of the equivalent SDOF system are reported in Table 5.

Table 5. Dynamic parameters of the equivalent SDOF system.

m^*	k^*	ω^*	T^*
[kg 10^3]	[kN/m]	[rad/s]	[s]
224.76	**7113.36**	**5.6257**	**1.117**

Therefore, the characteristic points of the capacity curve are defined in the planes $\alpha - \delta$, $F_b - d_c$, $F^* - D^*$, $S_\alpha - S_D$ assessing the capacity in terms of accelerations for the Nassar and Krawinkler approach and ADRS spectrum approach. In particular, in Table 6, the results based on the use of the ADRS spectrum, and in Table 7, the results based on the use of the Nassar and Krawinkler formulation, are reported.

Table 6. ADRS spectrum approach.

	FO	O	LS	NC
F **[kN]**	1284.84	2009.08	2009.08	2009.08
F* **[kN]**	893.41	1397.01	1397.01	1397.01
d **[m]**	0.1802	0.2824	0.5901	0.5901
d* **[m]**	**0.1253**	**0.1964**	**0.4103**	**0.4103**
Sa* **[g]**	**0.404**	**0.634**	**1.324**	**1.324**

Table 7. Nassar and Krawinkler approach.

	FO	O	LS	NC
F [kN]	1284.84	2009.08	2009.08	2009.08
F^* [kN]	893.41	1397.01	1397.01	1397.01
d [m]	0.1802	0.2824	0.5901	0.5901
d^* [m]	0.1253	0.1964	0.4103	0.4103
μ [m]	–	–	2.089	2.089
Sa^* [g]	0.405	0.634	1.353	1.353

Seismic performance verification requires that, for each limit state, the inequality $S_{\alpha.ls}(T^*)_{capacity} \geq S_{\alpha.ls}(T^*)_{demand}$ is satisfied.

5.3. Global Moment Resisting Frame

Global moment resisting frames are designed according to the TPMC. The design results are reported in Figure 8.

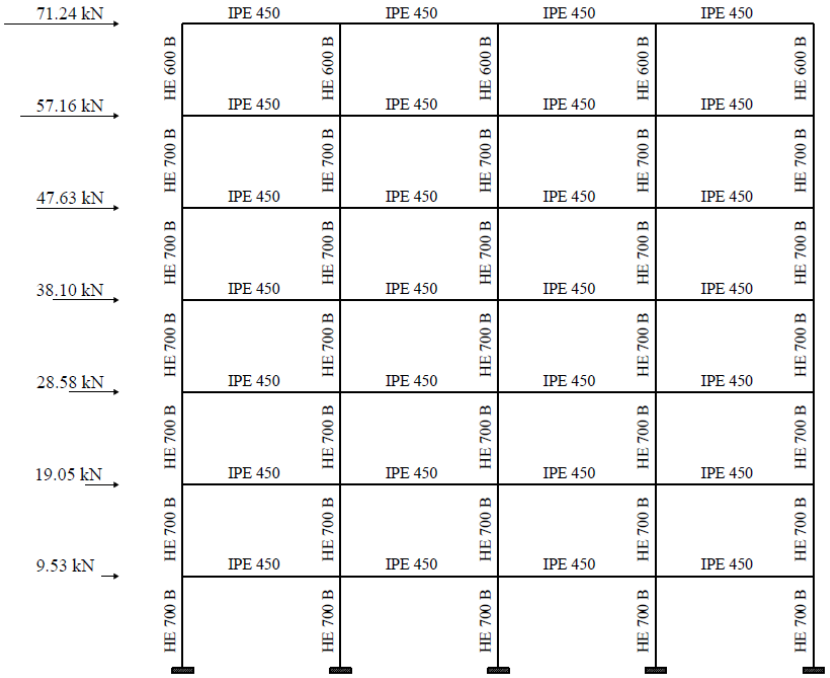

Figure 8. Diagram of the frame constituting the numeric example with the indication of beams, columns and seismic forces.

The trilinear capacity curve is shown in Figure 9, which also shows the characteristic performance points of the model.

Parameters obtained from the elastic analysis:

- $\delta_1(\alpha = 1) = 0.02684\ m$
- $k = 37.2606\ m^{-1}$
- $\delta_A = \delta_y = 0.1602\ m$
- $\alpha_A = \alpha_y = k\delta_y = 5.999$

Parameters obtained from the rigid-plastic analysis:

- $\alpha_0 = 10.149$
- $\gamma_s = 0.53\ m^{-1}$
- $\alpha = \alpha_0 - \gamma_s(\delta - \delta_y) \rightarrow \alpha = 10.149 - 0.53(\delta - 0.1602)$
- $\alpha(\delta = 0) = \alpha_0 + \gamma_s\delta_y = 10.234$
- $H_0 = 24.5\ m$ (Global collapse mechanism)

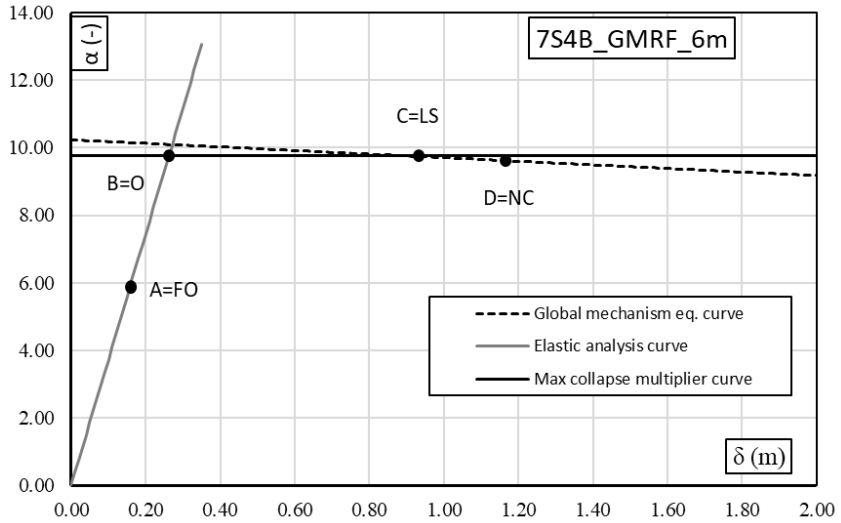

Figure 9. Trilinear model and characteristic points for the structure 7S4B_GMRF_6m.

Evaluation of the maximum multiplier using the calibrated Merchant−Rankine formula:

- $$\alpha_{max} = \frac{\alpha_0}{1 + \Psi \alpha_0 \gamma_s \delta_1} = 9.7594$$

where:

$$\Psi = 0.28488 - 0.14042\,\xi = 0.2763 \text{ with } \xi = \frac{\sum \frac{EI_b}{L_b}}{\sum \frac{EI_c}{L_c}} = 0.06129$$

and consequently $\delta_B = \frac{\alpha_{max}}{k} = 0.2619$ and $\delta_C = \delta_{mecc} = \frac{\alpha_0 - \alpha_{max}}{\gamma_s} + \delta_y = \frac{10.149 - 9.7594}{0.53} + 0.1602 = 0.8946\ m$.

Evaluation of the plastic rotation demand corresponding to the development of the collapse mechanism for the first plasticized element (first storey beams):

- $$\theta_{p.mec} = \frac{n_s \delta_y}{H_0}\left[\frac{\Psi_1}{\Psi_2}\Psi_3\left(\frac{\alpha_{max}}{\alpha_y} - 1\right)^{\Psi_4}\frac{1 - \Psi_5\gamma_s}{1 - \Psi_6\gamma_s}\right] = 0.01886 \text{ rad}$$

The calculation of the corresponding capacity provides a final plastic rotation value of $8\theta_y = 8 \times 0.008257 = 0.06605$ rad.

Evaluation of the plastic rotation demand corresponding to the development of the collapse mechanism for the critical element (the mechanism is global, so the critical element is one of the first storey columns):

- $$\theta_{p.mec} = \frac{n_s \delta_y}{H_0}\left[\frac{\Psi'_1}{\Psi'_2}\Psi'_3\left(\frac{\alpha_{max}}{\alpha_y} - 1\right)^{\Psi'_4}\frac{1 - \Psi'_5\gamma_s}{1 - \Psi'_6\gamma_s}\right] = 0.01774 \text{ rad}$$

The calculation of the corresponding capacity, in the case of the third storey columns, provides a value of the ultimate plastic rotation equal to $8\theta_y = 8 \times 0.003714 = 0.02971$ rad. Therefore, the ultimate conditions are governed by the columns of the first storey.

Considering the plastic rotation capacity, the ultimate displacement is given by:

$$\delta_u = \delta_C + (\vartheta_{p.u} - \vartheta_{p.mecc}) H_0 = 0.8946 + (0.02971 - 0.01774) \times 24.5 = 1.188\ m$$

All the verification procedures considered the use of the transformation of the MDOF system by means of the participation coefficient of the main vibration mode Γ. For this reason, it is necessary to define:

- The eigenvector $\underline{\phi} = \{\phi_1, \phi_2, \phi_3, \phi_4, \phi_5, \phi_6\}$ that, assuming $\phi_k = \frac{F_k}{F_n}$, is:

$$\phi_1 = 0.134\,\phi_2 = 0.267\,\phi_3 = 0.401$$
$$\phi_4 = 0.535\,\phi_5 = 0.669\,\phi_6 = 0.802\,\phi_7 = 1.000$$

- The modal participation factor Γ:

$$\Gamma = \frac{\sum_{k=1}^{n} m_k \phi_k}{\sum_{k=1}^{n} m_k {\phi_k}^2} = 1.4381$$

being:

$$m_1 = 57.98 \times 10^3 \text{ kg } m_2 = 57.98 \times 10^3 \text{ kg } m_3 = 57.98 \times 10^3 \text{ kg}$$
$$m_4 = 57.98 \times 10^3 \text{ kg } m_5 = 57.98 \times 10^3 \text{ kg } m_5 = 57.98 \times 10^3 \text{ kg } m_7 = 61.94 \times 10^3 \text{ kg}$$

The dynamic parameters of the equivalent SDOF system are reported in Table 8.

Table 8. Dynamic parameters of the equivalent SDOF system.

m^*	k^*	ω^*	T^*
[kg 10^3]	[kN/m]	[rad/s]	[s]
224.76	**10108.5**	**6.7063**	**0.9369**

Therefore, the characteristic points of the capacity curve are defined in the planes $\alpha - \delta$, $F_b - d_c$, $F^* - D^*$, $S_\alpha - S_D$ assessing the capacity in terms of accelerations for the Nassar and Krawinkler approach and ADRS spectrum approach. In particular, in Table 9, the results based on the use of the ADRS spectrum, and in Table 10, results based on the use of the Nassar and Krawinkler formulation, are reported.

Table 9. European code approach.

	FO	O	LS	NC
F [kN]	1627.71	2647.66	2647.66	2647.51
F^* [kN]	1131.83	1841.05	1841.05	1840.94
d [m]	0.1602	0.2619	0.8946	1.1879
d^* [m]	**0.1114**	**0.1821**	**0.6220**	**0.8260**
Sa^* [g]	**0.511**	**0.835**	**2.852**	**3.787**

Table 10. Nassar and Krawinkler approach.

	FO	O	LS	NC_0
F [kN]	1627.71	2647.66	2647.66	2776.3
F^* [kN]	1131.83	1841.05	1841.05	1930.53
d [m]	0.1602	0.2619	0.8946	1.1879
d^* [m]	**0.1114**	**0.1821**	**0.6220**	**0.8260**
μ [m]	–	–	3.415	4.535
Sa^* [g]	**0.513**	**0.835**	**2.958**	**3.988**

Seismic performance verification requires that, for each limit state, the inequality $S_{\alpha.ls}(T^*)_{capacity} \geq S_{\alpha.ls}(T^*)_{demand}$ is satisfied.

6. Conclusions

In this paper, some numeric examples explaining the application of a new assessment method are reported. As can be seen from the given numerical examples, the methodology

is of easy and rapid application. The methodology is also completely analytical since the equations of the branches constituting the trilinear model can be obtained uniquely, given the horizontal seismic actions and the sections of beams and columns of the analyzed frame. The speed of application and the uniqueness show that this methodology is strongly indicated for the evaluation of seismic performances in the immediate post-earthquake or the large-scale assessment of the seismic vulnerability of the built heritage. Furthermore, it constitutes a suitable tool to check the capacity of the buildings designed with the new seismic code prescriptions. The reliability of the procedure is testified by the extensive regression analysis, carried out on 420 frames designed with different approaches. The feasibility of the procedure is very high and makes it suitable to be applied indiscriminately to frames belonging to different historical periods.

Table 11 shows a comparison between the results in terms of the percentage scatter between the values computed from pushover analysis and the proposed method of the maximum bearing multiplier α and the displacement corresponding to the collapse and formation of the plastic mechanism. It can be observed that the scatter is always lower than 10%, thus testifying the accuracy of the proposed formulations. Moreover, the results achieved by the simplified assessment procedure are on the safe side.

Table 11. Percentage scatter between the pushover analysis and the simplified approach.

	α_{max} [%]	δ_{mec} [%]	δ_u [%]
GMRF	0.9	1.9	5.3
SMRF	5.2	9.5	4.8
OMRF	1.8	5.1	7.2

The assessment of structure performances, in terms of comparing capacity-demand, has been performed using the Nassar and Krawinkler approach, characterized by a wide generality because it does not discriminate between high and low periods of vibration and accounts for second-order effects. Finally, is important to note that the discretization of the trilinear model in characteristic performance points makes it easy to compare the capacity and demand for each limit state given by codes.

Author Contributions: R.M.: Conceptualization, Methodology, Writing—Review & Editing, Supervision; E.N.: Software, Validation, Resources, Data Curation, Writing—Review & Editing, Supervision; V.P.: Conceptualization, Methodology, Writing—Review & Editing, Supervision; P.T.: Software, Validation, Writing—Original Draft, Investigation, Formal analysis. All authors have read and agreed to the published version of the manuscript.

Funding: The research leading to the results presented in this paper has received funding from the Italian Department of Civil Protection (DPC−Reluis).

Institutional Review Board Statement: Not applicable.

Informed Consent Statement: Not applicable.

Data Availability Statement: Not applicable.

Acknowledgments: The support of DPC−RELUIS 2019−2021 is gratefully acknowledged.

Conflicts of Interest: The authors declare no conflict of interest. The funders had no role in the design of the study; in the collection, analyses, or interpretation of data; in the writing of the manuscript, or in the decision to publish the results.

Notation:

Symbol	Description
α_y	Multiplier of horizontal forces corresponding to the formation of the first plastic hinge
α_0	Kinematically admissible multiplier of horizontal forces due to first−order rigid−plastic analysis
Γ	Modal participation factor.
γ_s	Slope of the mechanism equilibrium curve, evaluated for the specific structure
γ	Non−dimensional slope of the mechanism equilibrium curve
γ_{ov}	Overstrength coefficient
δ_1	Elastic top sway displacement, corresponding to the design value of the seismic forces
$1/\delta_1$	Slope of the elastic branch
δ_y	Top sway displacement corresponding to the formation of the first plastic hinge
δ_A	Minimum top−sway displacement between service conditions and formation of the first plastic hinge
$\theta_{p.u}$	Plastic hinge capacity assumed equal to 8.0 ϑ_y according to Eurocode 8−3 [26]
$\theta_{p.mec}$	Plastic hinge rotation demand corresponding to the formation of the collapse mechanism
θ_y	Chord rotation at yielding
μ_{ls}	Ductility for the specific limit state
ξ	Sensitivity factor for first storey members
Φ_k	k-th component of the first mode eigenvector
φ	Stability coefficient
Ψ_i	Regression coefficient for the first plasticized member—Evaluation of plastic rotation demand
Ψ'_i	Regression coefficient for the critical member—Evaluation of plastic rotation demand
α_i	Regression coefficient
b_i	Regression coefficient
E	Elastic modulus
F_{ls}	Base shear force corresponding to the specific limit state
H_0	Total height of the storeys involved in the collapse mechanism
I_b	Moment of inertia of the beam
I_c	Moment of inertia of the column
L_b	Length of the beam
L_c	Length of the column
l_m	Length of the member
I_m	Moment of inertia of the member
$M_{p.m.}$	Plastic moment of the member
n_s	Number of storeys
q	The ratio between the maximum structural bearing capacity and the yielding capacity
$S_{\alpha.ls}$	Spectral acceleration in terms of capacity linked to the considered limit state
$S_\alpha(T^*)$	Spectral acceleration demand, provided by the code, for the specific limit state.
$(\dots)^*$	Properties referred to the equivalent SDOF system—m^* (mass); T^* (Vibration period); ω^* (Pulse)

Abbreviations

Acronym	Description
GMRF	Global Moment Resisting Frames
SMRF	Special Moment Resisting Frames
OMRFs	Ordinary Moment Resisting Frames
TPMC	Theory of Plastic Mechanism Control
EC8	Eurocode 8
SDOF	Single Degree of Freedom
MDOF	Multiple Degree of Freedom
ADRS	Acceleration-Displacement Response Spectrum

References

1. Jung, H.-C.; Jung, J.-S.; Lee, K.S. Seismic performance evaluation of internal steel frame connection method for seismic strengthening by cycling load test and nonlinear analysis. *J. Korea Concr. Inst.* **2019**, *31*, 79–88. [CrossRef]
2. Brebbia, C. *Earthquake Resistant Engineering Structures X*; WIT Transactions on the Built Environment, Technology & Engineering: Southampton, UK, 2015.
3. Montuori, R.; Nastri, E.; Piluso, V. Problems of modeling for the analysis of the seismic vulnerability of existing buildings. *Ing. Sismica* **2019**, *36*, 53–85.
4. Nastri, E.; Vergato, M.; Latour, M. Performance evaluation of a seismic retrofitted R.C. precast industrial building. *Earthq. Struct.* **2017**, *12*, 13–21. [CrossRef]
5. Taiyari, F.; Formisano, A.; Mazzolani, F.M. Seismic Behaviour Assessment of Steel Moment Resisting Frames under Near-Field Earthquakes. *Int. J. Steel Struct.* **2019**, *19*, 1421–1430. [CrossRef]
6. Wang, S.; Lai, J.-W.; Schoettler, M.J.; Mahin, S.A. Seismic assessment of existing tall buildings: A case study of a 35-story steel building with pre-Northridge connection. *Eng. Struct.* **2017**, *141*, 624–633. [CrossRef]
7. Hwang, S.-H.; Jeon, J.-S.; Lee, K. Evaluation of economic losses and collapse safety of steel moment frame buildings designed for risk categories II and IV. *Eng. Struct.* **2019**, *201*, 10983. [CrossRef]
8. Formisano, A.; Landolfo, R.; Mazzolani, F.M. Robustness assessment approaches for steel framed structures under catastrophic events. *Comput. Struct.* **2015**, *147*, 216–228. [CrossRef]
9. Bojórquez, E.; López-Barraza, A.; Reyes-Salazar, A.; Ruiz, S.E.; Ruiz-García, J.; Formisano, A.; López-Almansa, F.; Carrillo, J.; Bojórquez, J. Improving the Structural Reliability of Steel Frames Using Posttensioned Connections. *Adv. Civ. Eng.* **2019**, *2019*, 8912390. [CrossRef]
10. Krawinkler, H.; Seneviratna, G.D.P.K. Pros and cons of a pushover analysis of seismic performance evaluation. *Eng. Struct.* **1998**, *20*, 452–464. [CrossRef]
11. Gupta, A.; Krawinkler, H. Feasibility of push-over analyses for estimation of strength demand, Stessa 2003. Behaviour of Steel Structures in Seismic Areas. In Proceedings of the 4th International Specialty Conference, Naples, Italy, 9–12 June 2003.
12. Fajfar, P. A Nonlinear Analysis Method for Performance-Based Seismic Design. *Earthq. Spectra* **2000**, *16*, 573–592. [CrossRef]
13. Gentile, R.; del Vecchio, C.; Pampanin, S.; Raffaele, D.; Uva, G. Refinement and Validation of the Simple Lateral Mechanism Analysis (SLaMA) Procedure for RC Frames. *J. Earthq. Eng.* **2009**. in Press. [CrossRef]
14. Bernuzzi, C.; Rodigari, D.; Simoncelli, M. Post-earthquake damage assessment of moment resisting steel frames. *Ing. Sismica* **2019**, *36*, 35–55.
15. Pengfei, W.; Shan, G.; Sheling, W.; Xiaofei, W. Anti-collapse equivalent dynamic analysis on steel moment frame. *Ing. Sismica* **2019**, *36*, 1–19.
16. Ferraioli, M.; Lavino, A.; Mandara, A. Effectiveness of multi-mode pushover analysis procedure for the estimation of seismic demands of steel moment frames. *Ing. Sismica* **2018**, *35*, 78–90.
17. Bernuzzi, C.; Chesi, C.; Rodigari, D.; De Col, R. Remarks on the approaches for seismic design of moment-resisting steel frames. *Ing. Sismica* **2018**, *35*, 37–47.
18. Pongiglione, M.; Calderini, C.; D'Aniello, M.; Landolfo, R. Novel reversible seismic-resistant joint for sustainable and deconstructable steel structures. *J. Build. Eng.* **2021**, *35*, 101989. [CrossRef]
19. Romano, E.; Cascini, L.; D'Aniello, M.; Portioli, F.; Landolfo, R. A simplified multi-performance approach to life-cycle assessment of steel structures. *Structures* **2020**, *27*, 371–382. [CrossRef]
20. Harirchian, E.; Kumari, V.; Jadhav, K.; Das, R.R.; Rasulzade, S.; Lahmer, T. A machine learning framework for assessing seismic hazard safety of reinforced concrete buildings. *Appl. Sci.* **2020**, *10*, 7153. [CrossRef]
21. Harirchian, E.; Jadhav, K.; Mohammad, K.; Hosseini, S.E.A.; Lahmer, T. A comparative study of MCDM methods integrated with rapid visual seismic vulnerability assessment of existing RC structures. *Appl. Sci.* **2020**, *10*, 6411. [CrossRef]
22. American Society of Civil Engineers. Seismic design criteria for structures, systems, and components in nuclear facilities. *ASCE Stand.* **2005**, i-81.
23. Montuori, R.; Nastri, E.; Piluso, V.; Todisco, P. A simplified performance based approach for the evaluation of seismic performances of steel frames. *Eng. Struct.* **2020**, *224*, 111222. [CrossRef]
24. Gupta, A.; Krawinkler, H. Seismic Demands for Performance Evaluation of Steel Moment Resisting Frame Structures. Ph.D. Thesis, Stanford University, Stanford, CA, USA, 1999.
25. Bruneau, M.; Uang, C.M.; Sabelli, R.S.E. *Ductile Design of Steel Structures*; McGraw-Hill: New York, NY, USA, 2011.
26. CEN. *Eurocode 8 EN 1998-3: Design of Structures for Earthquake Resistance—Part 3: Assessment and Retrofitting of Buildings*; CEN: Brussels, Belgium, 2004.
27. Nassar, A.A.; Krawinkler, H. *Seismic Demands for SDOF and MDOF Systems*; John A Blume Earthquake Engineering Center Technical Report 95; Stanford Digital Repository: Stanford, CA, USA, 1991.
28. Montuori, R.; Gabbianelli, G.; Nastri, E.; Simoncelli, M. Rigid plastic analysis for the seismic performance evaluation of steel storage racks. *Steel Compos. Struct.* **2019**, *32*, 1–19.
29. Montuori, R.; Nastri, E.; Piluso, V. Advances in theory of plastic mechanism control: Closed form solution for MR-Frames. *Earthq. Eng. Struct. Dyn.* **2015**, *44*, 1035–1054. [CrossRef]

30. Nastri, E.; D'Aniello, M.; Zimbru, M.; Streppone, S.; Landolfo, R.; Montuori, R.; Piluso, V. Seismic response of steel Moment Resisting Frames equipped with friction beam-to-column joints. *Soil Dyn. Earthq. Eng.* **2019**, *119*, 144–157. [CrossRef]
31. Piluso, V.; Montuori, R.; Nastri, E.; Paciello, A. Seismic response of MRF-CBF dual systems equipped with low damage friction connections. *J. Constr. Steel Res.* **2019**, *154*, 263–277. [CrossRef]
32. Krishnan, S.; Muto, M. Mechanism of collapse of Tall Steel Moment-Frame Buildings under Earthquake Excitation. *J. Struct. Eng. Asce* **2012**, *138*, 1361–1387. [CrossRef]
33. Piluso, V.; Pisapia, A.; Castaldo, P.; Nastri, E. Probabilistic Theory of Plastic Mechanism Control for Steel Moment Resisting Frames. *Struct. Saf.* **2019**, *76*, 95–107. [CrossRef]
34. Priestley, M.J.N. Performance based seismic design. *Bull. N. Z. Soc. Earthq. Eng.* **2000**, *33*, 325–346. [CrossRef]
35. CEN. *Eurocode 8 EN 1998-1: Design of Structures for Earthquake Resistance—Part 1: General Rules, Seismic Actions and Rules for Buildings*; CEN: Brussels, Belgium, 2004.
36. CEN. *Eurocode 3 UNI EN 1993-1-1: Design of Steel Structures Part 1-1: General Rules and Rules for Buildings*; CEN: Brussels, Belgium, 2005.
37. Mazzolani, F.M.; Piluso, V. Plastic Design of Seismic Resistant Steel Frames. *Earthq. Eng. Struct. Dyn.* **1997**, *26*, 167–191. [CrossRef]
38. Mazzolani, F.M.; Piluso, V. *Theory and Design of Seismic Resistant Steel Frames*; E & FN Spon: London, UK, 1996.
39. Yun, S.Y.; Hamburger, R.O.; Cornell, C.A.; Foutch, D.A. Seismic performance evaluation for steel moment frames. *J. Struct. Eng.* **2002**, *128*, 534–545. [CrossRef]
40. Grecea, D.; Dinu, F.; Dubina, D. Performance Criteria for MR Steel Frames in Seismic Zones. *J. Constr. Steel Res.* **2004**, *60*, 739–749. [CrossRef]
41. Newmark, N.M.; Hall, W.J. *Earthquake Spectra and Design*; EERI Monographs: Berkeley, CA, USA, 1982.
42. Ferraioli, M.; Lavino, A.; Mandara, A. An adaptive capacity spectrum method for estimating seismic response of steel moment-resisting frames. *Ing. Sismica* **2016**, *33*, 47–60.
43. Naeim, F. Earthquake Engineering-From Engineering Seismology to Performance-Based Engineering. *Earthq. Spectra* **2005**, *21*, 609–611. [CrossRef]